Available online at www.sciencedirect.com
ScienceDirect
Journal of Catalysis 245 (2007) 272–278
JOURNAL OF CATALYSIS
www.elsevier.com/locate/jcat

Highly selective Pd/titanate nanotube catalysts for the double-bond migration reaction

Laura Torrente-Murciano [a], Alexei A. Lapkin [a,*], Dmitry V. Bavykin [b], Frank C. Walsh [b], Karen Wilson [c]

[a] *Catalysis and Reaction Engineering Group, Department of Chemical Engineering, University of Bath, Bath BA2 7AY, UK*
[b] *Electrochemical Engineering Group, School of Engineering Sciences, University of Southampton, Highfield, Southampton SO17 1BJ, UK*
[c] *Department of Chemistry, University of York, York YO10 5DD, UK*

Received 9 August 2006; revised 13 October 2006; accepted 17 October 2006

Available online 17 November 2006

Abstract

Pd(II) and Pd(0) catalysts supported onto titanate nanotubes ($H_2Ti_3O_7$) were prepared by an ion-exchange technique. The catalysts are characterised by narrow size distribution of metal nanoparticles on the external surface of the nanotubes. Pd(II) catalysts show high selectivity toward double-bond migration reaction versus hydrogenation in linear olefins. The catalytic activity exhibits a volcano-type dependence on the metal loading, with the maximum activity observed at ca. 8 wt%. The Pd(II) was shown to be rapidly reduced to Pd(0) by appropriate choice of solvent. Prereduced Pd(0) catalysts were found to be less active toward double-bond migration and more selective toward hydrogenation. The DBM reaction was faster in protic solvents, such as methanol or ethanol.

Keywords: Titanate nanotubes; Double-bond migration; Olefin isomerisation

1. Introduction

The double-bond migration (DBM) reaction is known to be catalysed by both liquid and solid state acids and bases, transition metal salts, organometallic complexes of transition metals, as well as supported transition metals, especially Pd, Ru, and Rh. DBM often occurs as an unwanted side reaction of olefins, as in the case of Wacker-type oxidation by the Pd(II)-polyoxometalate catalytic pair [1], or in the hydrogenation of olefins [2–5]. The DBM reaction is also important in synthesis. Examples of synthetically useful DBM reactions include deconjugation of enons [6], transformation of allylic alcohols into carbonyls [7,8], production of higher olefins as part of the SHOP process [9], isomerisation of eugenol [10] and flavonoids [11], and conjugation of linoleic acid [12]. More significantly, a number of tandem or one-pot sequences of reactions involving DBM have been successfully demonstrated and, in the case of hydroformylation of internal olefins, commercialised [13–17].

Among the many examples of DBM catalysis, the most active, selective, and well-researched catalysts are almost exclusively homogeneous transition metal salts and organometallic compounds; examples include $PdCl_2$, $PdCl_2{\cdot}2C_6H_5CN$ [18], $RhCl_3{\cdot}3H_2O$ [19], $Ni[P(OEt)_3]_4$ [20], and $RuClH(CO)(PPh_3)_3$ [21]. Homogeneous catalysis in conventional solvent systems necessarily raises the problem of catalyst recovery. Loss of transition metals into the product stream at the ppm level is becoming prohibitive to commercialisation. This drawback can be overcome in some cases by working in a multiphase system with immiscible solvents, such as the $scCO_2$-ionic liquid couple, or "smart" solvents with controllable solvatation power [22]. However, there is significant interest in developing truly heterogeneous catalytic processes that facilitate catalyst recovery and involve simpler process engineering, leading to cleaner chemical syntheses.

A number of heterogeneous catalysts with double-bond migration activity have been reported. The nontransition metal

* Corresponding author. Fax: +44 1225 385713.
E-mail address: a.lapkin@bath.ac.uk (A.A. Lapkin).

0021-9517/$ – see front matter
doi:10.1016/j.jcat.2006.10.015

catalysts are either solid bases or acids. The earlier literature describes supported alkali metals [23] and a dispersed alkali hydroxide [6] as isomerisation catalysts. The DBM reaction was used to estimate the number of acid sites in the alumina catalyst [24] and to evaluate the activity of magnesium mixed oxide catalysts [25]; it was found that the DBM reaction was catalysed by strong Brønsted sites in some zeolites [26,27]. Silylated large-pore acidic zeolites were reported to be more selective toward double-bond migration versus dimerisation [9], and Keggin-type polyoxometalate salts were found to be active in the gas-phase DBM reaction [28]. More recently, hydrotalcites were found to be efficient in synthetic applications of the DBM reaction to produce high-value speciality molecules [10,29].

In the case of transition metal catalysts, including important reactions of hydrogenation of vegetable oils [5] and enantioselective reactions promoted by cinchona modifiers [2], DBM is often cited as an undesirable side reaction in hydrogenation [3,30,31]. There are also few reports of synthetically important DBM reactions. Rhodium supported on alumina or carbon catalysts were shown to selectively steer DBM toward a more stable higher substituted unsaturated carbon position in quinine and quinidine, whereas a commercial Pd(0)/C catalyst was inactive [32]. In a series of papers. Murzin et al. reported conjugation of linoleic acid catalysed by supported transition metals in work aimed at producing two specific isomers known for their health effects [12,33,34]. Supported ruthenium catalysts were found to be most active, stable, and selective [35].

Recently, we have reported preparation of Au, Pt, Ru, Ni, and Pd supported on a novel structured mesoporous material: multilayered titanate nanotubes [36]. For Ru, Pt, and Pd, the ion-exchange mechanism of deposition resulted in the formation of small (1.4–5 nm) metal nanoparticles with a narrow size distribution over a broad range of metal loadings (up to 10 wt%). In the case of Ru(III)/titanate catalyst, this resulted in the independence of catalyst activity (expressed as turnover frequency) on the metal loading, observed in the reaction of liquid-phase selective oxidation of alcohols [37]. It is interesting to investigate the activity of Pd/titanate nanotube catalysts in the DBM reaction, because of this reaction's sensitivity to the nature of the active sites. In most previous studies of heterogeneous Pd catalysts of DBM reaction, the metal deposited from a salt solution was reduced by hydrogen or formic acid before catalytic tests, generating Pd(0) catalytic species. It was also shown that unreduced, supported Pd catalysts exhibit higher selectivity toward double-bond migration than reduced catalysts, which tend to be more selective toward hydrogenation [38].

It is known that interaction with reducible supports, such as TiO_2, may promote generation of ionic metal species, which can be either beneficial or detrimental to catalytic activity, the so-called SMSI effect [39]. The nature of the titanate support and the ion-exchange preparation mechanism may allow the stabilisation of the ionic metal species and could give rise to high selectivity toward the DBM reaction. There is only one report in the open literature of a Pd/titanate nanotubes catalyst, prepared by reduction of $PdCl_2$ by glycol [40], that was found to be very active for the electrooxidation of methanol. This paper reports recent data on the selective double-bond migration reaction promoted by in situ generated active species of the mixed Pd(II)/Pd(0) catalyst supported on the external surface of ion-exchangeable, titanate nanotubes.

2. Experimental

2.1. Catalyst preparation and characterisation

The titanate nanotubes were prepared by a hydrothermal method described elsewhere [41]. In a typical synthesis, 20 g of TiO_2 (Fisher Chemicals) was added to 300 mL of 10 M NaOH solution and heated in an autoclave for 20 h at 413 K. After synthesis, the titanate nanotubes were washed several times with demineralised water. The powder was repeatedly washed with demineralised water and 0.1 M H_2SO_4 until the pH of the wash was approximately 7. The samples were dried overnight at 393 K.

Palladium(II) was deposited by ion exchange from aqueous palladium chloride solutions of different concentrations. HCl was added to palladium chloride solutions to avoid precipitation of palladium black. The initial pH of the solution depended on the salt and HCl concentration. For example, in the case of the 8.86 wt% catalyst, the initial pH of salt-HCl solution was 1.9; the final pH was about 4. Titanate powder was added to the solution under vigorous stirring and left at ambient temperature for 2 h. After ion exchange, the catalyst colour changed from white to orange-brown, depending on the palladium concentration. Samples were filtered and washed with the minimum quantity of demineralised water. The remaining solutions were analyzed by atomic absorption spectroscopy (Perkin Elmer) to determine the quantity of deposited palladium. Some catalysts were left in the "as prepared" condition, and others were reduced at room temperature by reaction with aqueous $NaBH_4$. After preparation, all catalysts were dried at 393 K.

XPS measurements were performed using a Kratos Axis HSi instrument equipped with a Mg$K\alpha$ X-ray source and charge neutraliser. Spectra were acquired using a pass energy of 20 eV with an X-ray power of 169 W. Spectra were energy-referenced using valence band and adventitious carbon, whereas quantification and deconvolution was performed using CASA-XPS version 2.3.9 software. TEM images were obtained using JEOL 3010 electron microscope. The solid power samples were deposited on a perforated copper grid coated with gold. XRD spectra were recorded using a Bruker AXS D8 Discoverer X-ray diffractometer, with CuK_α radiation $\lambda = 0.154$ nm and a graphite monochromator, in the 2θ range of 5°–75°.

2.2. Catalytic tests and materials

The performance of Pd(II) and Pd(0) supported onto titanate nanotubes catalysts was tested in the reaction of isomerisation of allylbenzene (**I**). This is a simple reaction with a narrow product distribution. The double-bond migration produces *trans*-phenyl propene (**II**) as the desired product (the *cis*-isomer is <5% in equilibrium, and its formation is unfavourable), the

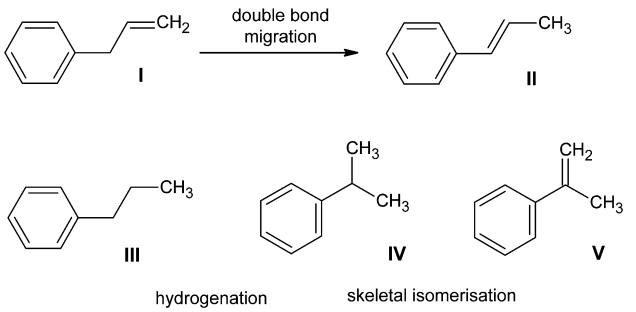

Fig. 1. Potential products (**II**–**V**) of reaction of allylbenzene (**I**) in the presence of an isomerisation catalyst.

skeletal isomerisation produces α-methyl styrene (**V**), and hydrogenation produces propylbenzene (**III**) and cumene (**IV**) (see Fig. 1).

Allylbenzene, *trans*-phenyl propene, and propylbenzene (99% purity), along with methanol, ethanol, *N*-methylpyrrolidone (NMP), and *n*-hexane, were obtained from Sigma-Aldrich. Reactions were performed in a 100-mL, three-necked glass flask under reflux. The initial concentration of allylbenzene was 0.002 M in most experiments. In a typical experiment, solvent and reactants were preheated to reaction temperature (348 K in the case of ethanol, and 333 K with methanol, *n*-hexane, and NMP). Once temperature was stabilised, the reaction was initiated by adding 200 mg of a catalyst. Samples (1 mL) were periodically withdrawn from the reactor. These samples were filtered with 0.2 μm nylon filters and analyzed by gas chromatography (Varian 3800) using a capillary column (Alltech, EC-WAX) and a flame ionization detector (FID). The catalysts were recovered after reaction by filtration for XPS analysis. The material balance was closed in all reactions to within ±10%, and the accuracy of determination of concentrations was better than ±6%. Turnover frequency (TOF) was calculated per unit amount (mol) of Pd, disregarding the oxidation state and the mean metal particle surface area.

3. Results and discussion

3.1. Preparation and characterisation of catalysts and titanate nanotubes

Their high ion-exchange capacity and open pore mesoporous structure makes titanate nanotubes good supports for metal nanoparticles [36]. The powder XRD pattern of the nanotubes, shown in Fig. 2, corresponds well with the reflections of a trititanate $H_2Ti_3O_7$, which is believed to be the most likely structure of the nanotubes [36]. This confirms that the starting material is the same as that used in the study of a supported Ru(III) catalyst [42] and that the nanotubes had not been significantly affected by rapid washing with sulfuric acid.

The isotherm of adsorption of palladium onto titanate nanotubes was determined at room temperature by measuring the initial and equilibrium palladium concentrations in the stock solutions (Fig. 3). The ion-exchange deposition method results in high loadings (up to 10.1 wt%) of palladium metal nanoparticles supported on the surface of the nanotubes. This also

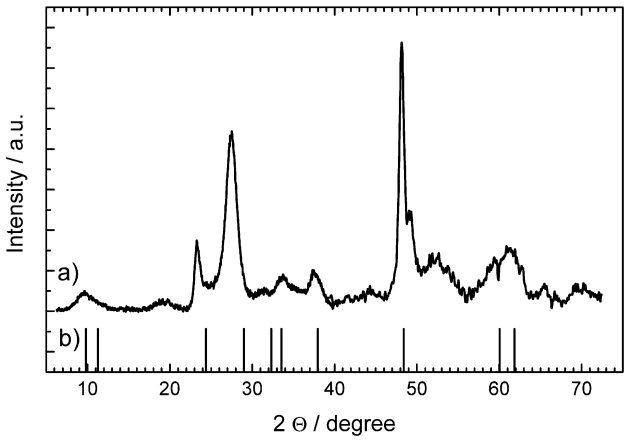

Fig. 2. XRD pattern of titanate nanotubes: (a) 'as prepared' powder, (b) reflections of the trititanate [42].

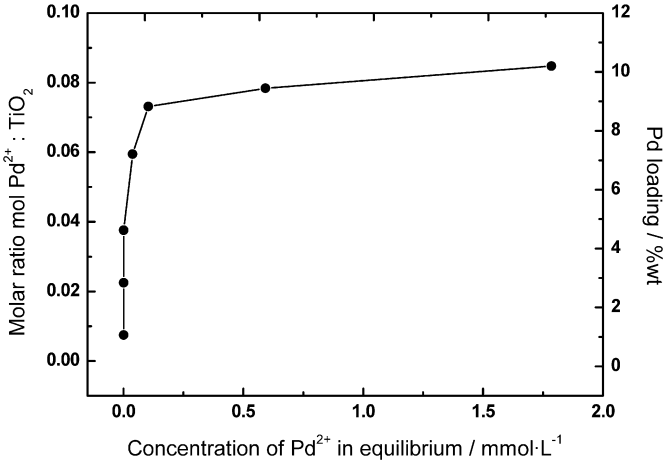

Fig. 3. Isotherm for adsorption of palladium from an aqueous $PdCl_2$ solution onto titanate nanotubes at 298 K.

indicates the high degree of palladium proton exchange; for example, the reaction of Pd(II) with protons in the titanate nanotubes from a 2 mM solution of $PdCl_2$ results in a Pd^{2+}/Ti ratio of 0.08, whereas a maximum value 0.33 would correspond to $PdTi_3O_7$. In other words, almost 25% of all protons in the titanate nanotubes can be replaced by Pd(II) from relatively dilute solution of a salt. The isotherm of adsorption is characterised by a very sharp increase in metal loading with a small increase in the concentration of the stock solution; nearly quantitative sorption of Pd(II) results in negligible residual equilibrium concentration in solution, as shown in Fig. 3. Such a small equilibrium concentration of Pd(II) in water suspension of palladium-exchanged titanate nanotubes should result in a negligible rate of palladium leaching from the catalysts.

The TEM images of titanate nanotubes decorated with palladium nanoparticles for various metal loadings are shown in Fig. 4. The distribution of Pd particles for the 4.75 wt% sample is not uniform; areas of nanotubes with a low density of Pd particles are accompanied by areas with a much higher density. The deposition of metal particles is more uniform for the samples with 6.97 and 8.86 wt% Pd loading. However, the size and shape of metal particles are very similar in all metal loadings

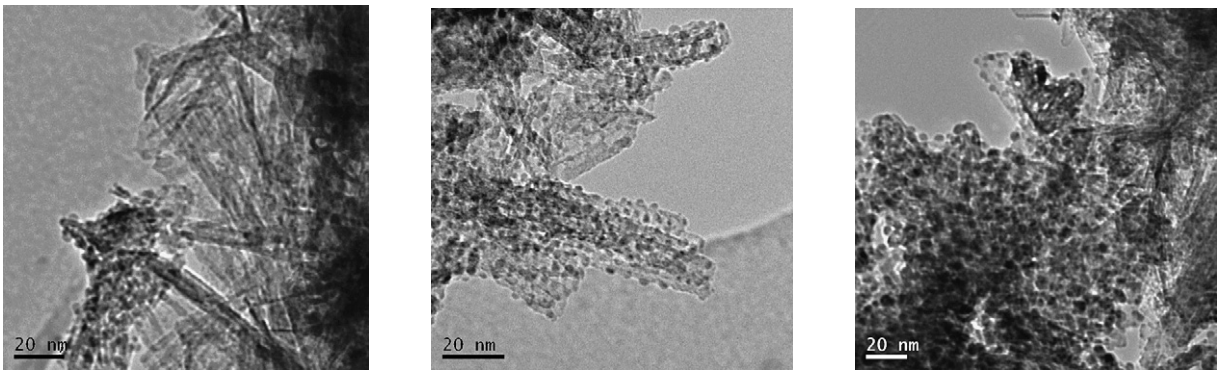

(a) (b) (c)

Fig. 4. TEM images of as 'prepared' Pd(II)/titanate nanotubes catalysts: (a) 4.75 wt% Pd, (b) 6.97 wt% Pd, (c) 8.86 wt% Pd.

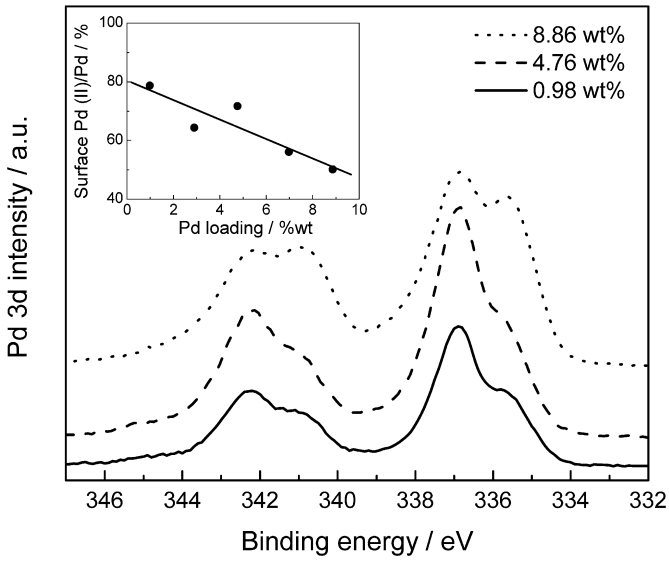

Fig. 5. XPS spectra of 'as prepared' Pd(II)/titanate nanotubes catalyst having different Pd loadings.

tested, with particle sizes of 1.9–4.8 nm and a slightly flattened, spheroidal metal particle shape. A similar, nonuniform deposition has also been found in the case of Pt/titanate nanotubes catalysts [36]. The nonuniform deposition of Pd at low metal loadings may be due to nonuniformity of the nanotube sample; the parts of a sample with higher surface energy react first, leaving the remaining nanotubes bare. However, it is also feasible that nonuniformity in metal deposition may be due to the ion-exchange method used; that is, in very fast ion exchange, the addition of dry titanate powder to the salt solution results in significant metal deposition onto the first portion of the sample that reaches the liquid phase. This is quite feasible; monitoring of pH during ion exchange has shown that 95% of pH change occurs in the first 8 min of reaction. Under different preparation conditions, such as vigorous stirring and slow addition of diluted metal salt solution (or simultaneous addition of metal salt and the nanotube powder/dispersion), the uniformity could be improved through reduction in the external mass transfer limitation. This is currently under investigation.

Fig. 5 shows the Pd 3d XP spectra for the series of Pd/titanate nanotubes samples with 0.98–8.86 wt% loading. The spectra can be deconvoluted into 2 components with Pd $3d_{5/2}$ binding energies of 337.1 and 335.5 eV, which are consistent with Pd(II) and Pd(0), respectively. Fig. 5, inset, shows that the percentage of the Pd(II) component decreases with the bulk Pd content, which is consistent with the Pd clusters becoming more metallic at higher loadings. Quantitative analysis of the XP spectra revealed that the surface Pd loadings for the series of catalysts were in the range of 18–42 wt%, somewhat higher than the bulk Pd content. Such observations are consistent with attenuation of the underlying Ti 2p signal occurring through exclusive coating of the external surface of the nanotubes with Pd, which is in accordance with the observations from TEM.

3.2. Catalytic results

Catalytic tests were performed with both prereduced catalysts and as-prepared catalysts assumed to contain a significant proportion of Pd(II) species, as confirmed by XPS. Reactions performed at 323 K showed no conversion; the following reactions were carried out at 348 K. Typical reaction profiles obtained with Pd(II)/titanate nanotubes and Pd(0)/titanate nanotubes catalysts are shown in Fig. 6. In all reactions with the Pd(II)/titanate catalysts, the main reaction was the double-bond migration to trans-phenyl propene. Dimerisation (based on the retention time, the unidentified product shown in Fig. 6 was assumed to be a dimer) and hydrogenation products were also formed in much smaller concentrations. Reaction proceeded without induction time until a ca. maximum 80% yield of the main desired product (Fig. 6a) was achieved and no skeletal isomers were found. Both the rate of reaction and selectivity were considerably lower for the prereduced Pd(0)/titanate catalysts (Fig. 6b). This suggests that the active species responsible for the double-bond migration reaction are not Pd(0), or else the catalyst could be poisoned by impurities of sodium and boron from a $NaBH_4$ reagent.

Varying the initial concentration of reactant (allylbenzene) between 0.001 and 0.01 M resulted in different conversions and selectivities (see Table 1). In all cases, a high selectivity of around 90% of the double-bond migration product was obtained at high conversions. Lower selectivity was observed in reaction with the lowest initial reactant concentration and the highest catalyst/reactant ratio (Fig. 7). In this case, almost 100% con-

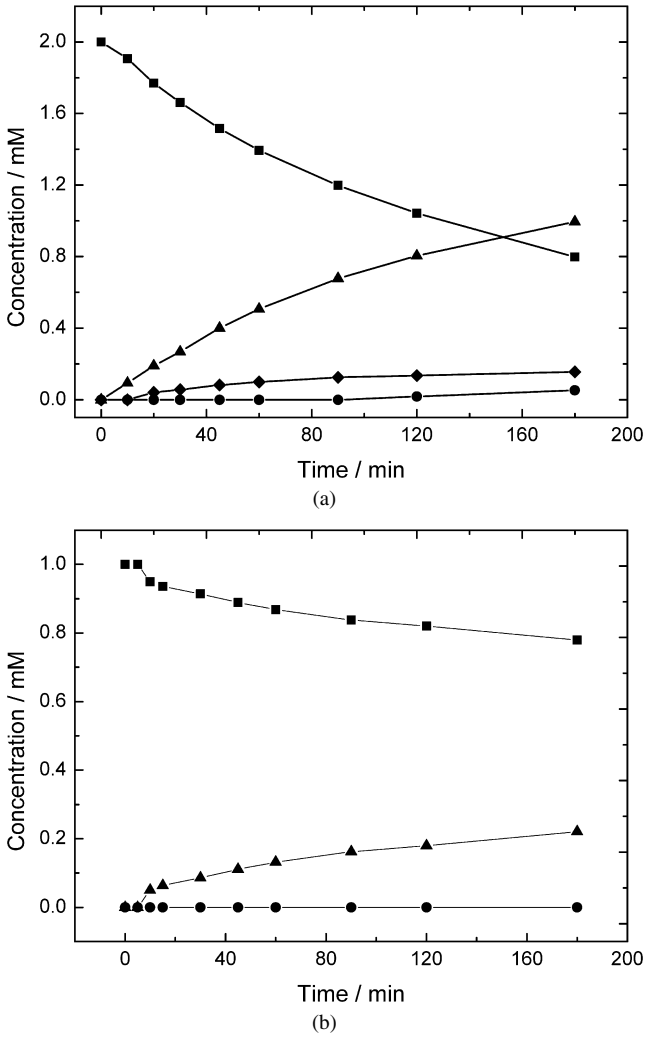

Fig. 6. Isomerisation reaction profiles in MeOH at 333 K. (a) Using a 6.97 wt% Pd(II)/titanate nanotubes. (b) Using a 7.33 wt% Pd(0)/titanate nanotubes prereduced in an aqueous solution of $NaBH_4$. (■) Allylbenzene, (▲) *trans*-phenyl propene, (●) propylbenzene and (◆) unidentified.

Table 1
Conversions and selectivities obtained with different reactant concentrations using 6.97 wt% Pd(II)/titanate nanotubes catalyst. Reaction conditions: allylbenzene reactant in ethanol solvent at 348 K

Initial conc. ($mol\,L^{-1}$)	Conversion (%)		Selectivity (%)	TOF @ 30 min (h^{-1})	Initial rate ($10^{-6}\,mol\,s^{-1}\,g^{-1}$)
	At 30 min	At 3 h			
0.001	68	100	69	1.0	2.7
0.002	74	96	93	2.3	5.9
0.005	13	33	86	1.1	2.8
0.01	5	12	86	0.8	2.0

version of allylbenzene was achieved in 2 h of reaction time. The considerable extent of hydrogenation reaction decreased the selectivity. The concentration versus time profile of *trans*-phenyl propene suggests a consecutive reaction mechanism; the decreased main product concentration appeared to coincide with an increase rate of hydrogenation byproduct formation. Data showing the dependence of selectivity on conversion (see below) suggest that double-bond migration and hydrogenation are parallel mechanisms and that the apparent acceleration of

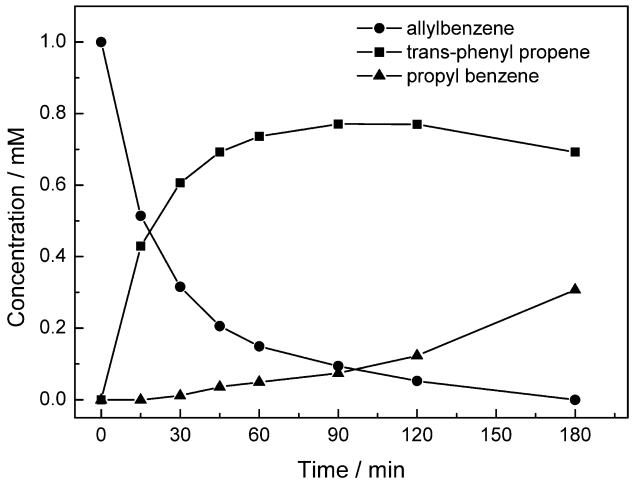

Fig. 7. Reaction profile for an initial allylbenzene reactant concentration of 0.001 M using a 6.97 wt% Pd(II)/titanate nanotubes catalyst, in ethanol at 348 K.

Table 2
Activity and selectivity data on Pd(II)/titanate nanotubes for isomerisation reaction. Reaction conditions: initial concentration of allylbenzene 0.002 M, in ethanol at 348 K

Pd (wt%)	Conversion (%)		Selectivity (%)	TOF @ 30 min (h^{-1})	Initial rate ($10^{-6}\,mol\,s^{-1}\,g^{-1}$)
	At 30 min	At 3 h			
2.90	28	68	77	2.2	5.7
6.97	74	96	93	2.3	5.9
8.86	77	98	86	1.8	4.8
10.13	61	86	88	1.3	3.3

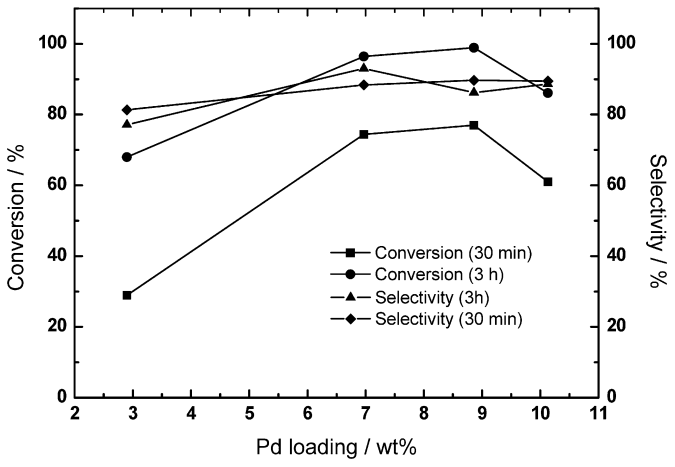

Fig. 8. Conversion and selectivity at different loadings of palladium on titanate nanotubes. Reaction conditions: initial concentration of allylbenzene reactant 0.001 M, in ethanol at 348 K.

the hydrogenation reaction relates to the generation of active catalytic sites for hydrogenation during the course of reaction.

The influence of metal loading on activity and selectivity is shown in Table 2. The conversion as a function of Pd(II) loading follows a typical volcano plot, as shown in Fig. 8, with the maximum at ca. 8–9 wt% Pd. Selectivity was found to be a weak function of metal loading and varied between 80 and 90%. This can be explained by the similar particle sizes of the metal ob-

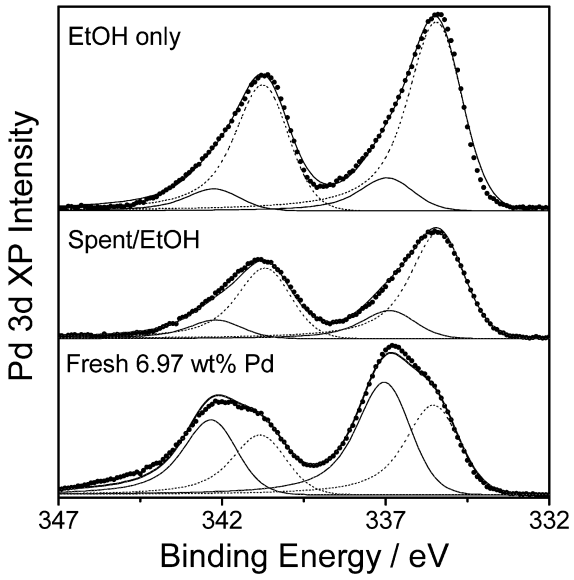

Fig. 9. XPS analysis of Pd(II)/titanate nanotubes catalysts with a 6.97 wt% Pd loading: equilibrated in ethanol: under reaction conditions (top), after reaction (middle) and fresh 'as prepared' catalyst (bottom).

served on TEM for catalysts with 5–9 wt% metal loading (see Fig. 4) and also corresponds well with the hypothesis of parallel hydrogenation and isomerisation reactions.

In all reactions, the orange-brown catalysts became completely black within the first 5 min. This colour change was due to the reduction of Pd(II) into Pd(0) as confirmed by XPS. XPS analysis of the fresh catalyst after a blank reaction (using ethanol as solvent) and after the double-bond migration reactions were performed to determine the oxidation state of palladium in all cases. Fig. 9 shows the Pd 3d region, revealing a mixture of Pd(II) and Pd(0) in the fresh catalysts, as indicated by the Pd $3d_{5/2}$ components at 337.1 and 335.5 eV, respectively. The initial catalyst started off with ∼56% of the Pd present as Pd(II); however, the Pd(II) component decreased to 12.5% after exposure to EtOH and to 18.3% after the isomerisation reaction. The corresponding increase in the relative intensity of 335.5 was attributed to Pd(0), indicating that catalyst reduction occurred.

Comparing our results on catalyst activity and selectivity with the literature data is difficult. The reported initial overall rate and TOF of Pd(0)/C in the isomerisation of linoleic acid are approximately 1.7×10^{-5} mol s^{-1} g^{-1} and 2.6 h^{-1}, respectively [35], slightly higher than the values found in this study. But the isomerisation of linoleic acid and allylbenzene are very different reactions, and these results do not permit direct comparison of the catalysts. Gas-phase isomerisation of allylbenzene over mixed-oxide base catalysts [43] was reported in units that do not allow comparison.

3.3. Influence of solvent

Different solvents were evaluated for the double-bond migration reaction (Table 3). For the same palladium loading on titanate nanotubes (6.97 wt%), a high conversion was obtained when an alcohol was used as solvent (ethanol or methanol),

Table 3
Influence of the solvent on the activity and selectivity of 6.97 wt% Pd(II)/titanate nanotubes catalyst for isomerisation of allylbenzene with an initial reactant concentration of 0.002 M

Solvent	Temperature (K)	Conversion (%)		Selectivity (%)
		At 30 min	At 3 h	
Ethanol	350	74	96	93
MeOH	333	16	60	82
MeOH:EtOH	333	20	49	85
NMP	350	0	0	0
Hexane	333	3	16	100

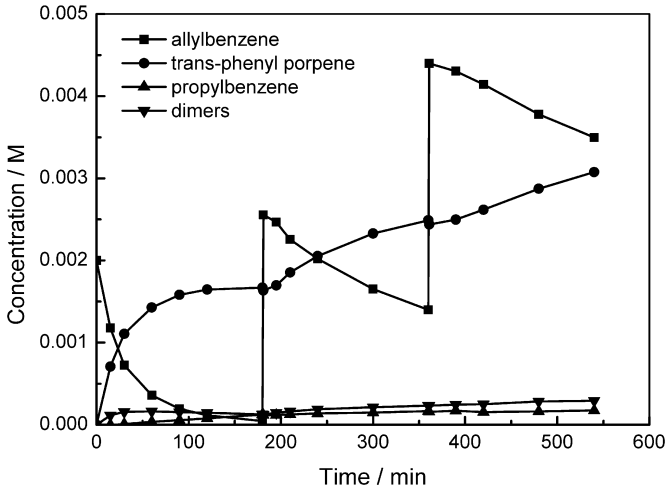

Fig. 10. Concentration profiles in three consecutive runs. Reaction conditions: 0.2 g of 10.1 wt% Pd(II)/titanate nanotubes catalyst; initial concentration of allylbenzene 0.002 M, in ethanol at 350 K.

with a higher value in the case of ethanol. When nonpolar solvents, *n*-hexane and NPM, were used, much lower conversions were obtained than in the case of the protic solvents or even null.

The solvent is clearly important, with ethanol and methanol promoting rapid reduction of Pd(II), as evidenced by the colour changes in the catalyst samples and detected by XPS (see Fig. 9). The change in catalyst colour occurred much more slowly when *n*-hexane or NPM was used than when alcohols were used. In the case of reduced metal catalysts, the effects of solvent have been attributed to the competitive sorption of solvent molecules on the active metal [2,44], with ethanol considered a special case. In Pd(II)/titanate nanotube catalysts, the role of the solvent is different, however. Clearly, alcohols as solvents promote the main reaction and at the same time result in the fastest reduction of Pd(II) species on the support.

3.4. Catalyst stability

No leaching of Pd was detected through atomic absorption measurements of the filtered reaction solutions. Catalyst stability and reusability were tested by adding fresh reactant to the reaction mixture after completion of reaction; the reaction profiles are shown in Fig. 10. Taking into account the dilution factor, the initial rates in the three consecutive reactions were 4.8×10^{-6}, 1.3×10^{-6}, and 7.2×10^{-7} mol s^{-1} g^{-1}. The apparent decrease

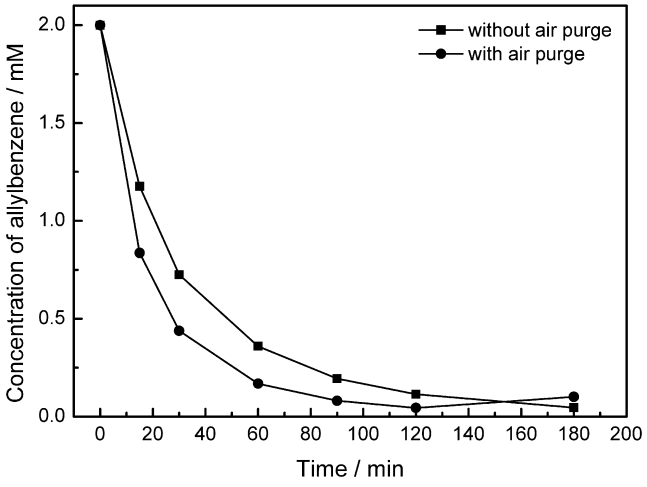

Fig. 11. Reactant concentration profiles with and without bubbling air into the reaction medium. Reaction conditions: catalyst: 0.2 g of 10.1 wt% Pd(II)/titanate nanotubes catalyst; initial concentration of allylbenzene 0.002 M, in ethanol at 350 K.

in the rate of reaction is probably due to the irreversible reduction of Pd(II) into the less active Pd(0) species. Direct oxidation of Pd(0) by oxygen has been suggested as a method of in-situ catalyst regeneration. The results obtained with and without air purge during the reaction are shown in Fig. 11. A higher initial reaction rate was found when the reaction was performed in the presence of air likely due to a temporary stabilisation of the active species by oxygen. Consecutive addition of fresh reagent after completion of the reaction resulted in the same reaction rate as seen in the absence of oxygen.

4. Conclusion

Catalysts containing Pd(II) supported on multilayered titanate nanotubes with a high loading of metal particles of small size and a narrow particle distribution were synthesised. After reduction in situ by methanol or ethanol solvents, the Pd(II)/titanate nanotube catalysts had high activity and very high selectivity toward double-bond migration during the isomerisation of allylbenzene. Reaction in the presence of oxygen promoted stability of the active catalyst. Other solvents, such as *n*-hexane and NMP, showed very low or zero activity. Ex situ reduction of the catalysts resulted in a loss of selectivity and activity toward isomerisation.

Acknowledgment

EPSRC funding of experimental studies at the University of Bath (grant GR/S86112/01) is gratefully acknowledged.

References

[1] A. Lambert, E.G. Derouane, I.V. Kozhevnikov, J. Catal. 211 (2002) 445–450.
[2] K. Borzeky, T. Mallat, A. Baiker, Catal. Lett. 59 (1999) 95–97.
[3] R.J. Grau, P.D. Zgolicz, C. Gutierrez, H.A. Taher, J. Mol. Catal. A Chem. 148 (1999) 203–214.
[4] G.V. Smith, J.A. Roth, D.S. Desai, J.L. Kosco, J. Catal. 30 (1973) 79–85.
[5] M.M.P. Zieverink, M.T. Kreutzer, F. Kapteijn, J.A. Moulijn, Ind. Eng. Chem. Res. 44 (2005) 9668–9675.
[6] E. D'Incan, P. Viout, Tetrahedron 40 (1984) 3421–3424.
[7] R. Uma, C. Crévisy, R. Grée, Chem. Rev. 103 (2003) 27–51.
[8] R.C. van der Drift, E. Bouwman, E. Drent, J. Organometallic Chem. 650 (2002) 1–24.
[9] D.M. Hamilton, US4727203 (1988), S.O. Company, USA.
[10] D. Kishore, S. Kannan, Appl. Catal. A Gen. 270 (2004) 227–235.
[11] Y. Hoshino, N. Takeno, Bull. Chem. Soc. Jpn. 67 (1994) 2873–2875.
[12] A. Bernas, P. Laukkanen, N. Kumar, P. Mäki-Arvela, J. Väyrynen, E. Laine, B. Holmbom, T. Salmi, D.Y. Murzin, J. Catal. 210 (2002) 354–366.
[13] H. Klein, R. Jackstell, M. Beller, Chem. Commun. (2005) 2283–2285.
[14] A. Seayad, M. Ahmed, H. Klein, R. Jackstell, T. Gross, M. Beller, Science 297 (2002) 1676–1678.
[15] B. Schmidt, Eur. J. Org. Chem. (2003) 816–819.
[16] A.E. Sutton, B.A. Siegal, D.F. Finnegan, M.L. Snapper, J. Am. Chem. Soc. 124 (2002) 13390–13391.
[17] G. Dyker, H. Markwitz, Synthesis (1998) 1750–1754.
[18] G. Bond, I. Hellier, J. Catal. 4 (1965) 1–5.
[19] F.J. Harrod, J. Chalk, J. Am. Chem. Soc. 86 (1963) 1776–1779.
[20] B. Corain, G. Puosi, J. Catal. 30 (1973) 403–408.
[21] H. Wakamatsu, M. Nishida, N. Adachi, M. Mori, J. Org. Chem. 65 (2000) 3966–3970.
[22] B. Cornils, W.A. Herrmann, I.T. Horváth, W. Leitner, S. Mecking, H. Olivier-Boubigou, D. Vogt, Multiphase Homogeneous Catalysis, Wiley–VCH, New York, 2005.
[23] J.K. Hambling, UK Patent 1,007,325 (1962).
[24] C.S. John, A. Tada, L.V.F. Kennedy, J. Chem. Soc. Faraday Trans. I 74 (1978) 498–505.
[25] M.A. Aramendía, V. Borau, C. Jiménez, A. Marinas, J.R. Ruiz, F.J. Urbano, J. Mol. Catal. A Chem. 218 (2004) 81–90.
[26] J.N. Kondo, K. Domen, F. Wakabayashi, J. Phys. Chem. 101 (1997) 5477–5479.
[27] J.N. Kondo, K. Domen, F. Wakabayashi, Microporous Mesoporous Matter. 21 (1998) 429–437.
[28] M.A. Parent, J.B. Moffat, J. Catal. 177 (1998) 335–342.
[29] D. Kishore, S. Kannan, J. Mol. Catal. A Chem. 223 (2004) 225–230.
[30] G.V. Smith, J.A. Roth, D.S. Desai, J.L. Kosco, J. Catal. 30 (1973) 79–85.
[31] P.V.D. Plank, J. Catal. 26 (1972) 42–50.
[32] D.E. Portlock, D. Naskar, L. West, W.L. Seibel, T. Gu, H.J. Krauss, X.S. Peng, P.M. Dybas, E.G. Soyke, S.B. Ashton, J. Burton, Tetrahedron Lett. 44 (2003) 5365–5368.
[33] A. Bernas, N. Kumar, P. Mäki-Arvela, N.V. Kul'kova, B. Holmbom, T. Salmi, D.Y. Murzin, Appl. Catal. A Gen. 245 (2003) 257–275.
[34] A. Bernas, N. Kumar, P. Laukkanen, V. Váyrynen, T. Salmi, D.Y. Murzin, Appl. Catal. A Gen. 267 (2004) 121–133.
[35] A. Bernas, N. Kumar, P. Mäki-Arvela, B. Holmbom, T. Salmi, D.Y. Murzin, Org. Proc. Res. Dev. 8 (2004) 341–352.
[36] D.V. Bavykin, A.A. Lapkin, P.K. Plucinski, L. Torrente-Murciano, J.M. Friedrich, F.C. Walsh, Top. Catal. 39 (2006); doi:10.1007/s11244-006-0051-4.
[37] D.V. Bavykin, A.A. Lapkin, P.K. Plucinski, J.M. Friedrich, F.C. Walsh, J. Catal. 235 (2005) 10–17.
[38] A. Bernas, N. Kumar, P. Mäki-Arvela, N.V. Kul'kova, B. Holmbom, T. Salmi, D.Y. Murzin, Appl. Catal. A Gen. 245 (2005) 257–275.
[39] M. Bowker, P. Stone, P. Morrall, R. Smith, R. Bennett, N. Perkins, R. Kvon, C. Pang, E. Fourre, M. Hall, J. Catal. 234 (2005) 172–181.
[40] M. Wang, D.-J. Guo, H.-L. Li, J. Solid State Chem. 178 (2005) 1996–2000.
[41] D.V. Bavykin, V.N. Parmon, A.A. Lapkin, F.C. Walsh, J. Mater. Chem. 14 (2004) 3370–3377.
[42] D.V. Bavykin, A.A. Lapkin, P.K. Plucinski, J.M. Friedrich, F.C. Walsh, J. Catal. 235 (2005) 10–17.
[43] M.A. Aramendía, V. Borau, C. Jiménez, A. Marinas, J.M. Marinas, F.J. Urbano, J. Catal. 211 (2002) 556–559.
[44] A. Bernas, P. Mäki-Arvela, N. Kumar, B. Holmbom, T. Salmi, D.Y. Murzin, Ind. Eng. Chem. Res. 42 (2005) 718–727.